

27 **Nomenclature**28 a_0 = initial crack length29 a_i = crack length at the i th loading point30 Δa_i = crack extension length at the i th loading point = $a_i - a_0$ 31 a_f = final crack length32 Δa_f = final crack extension length33 a_{fM} = measured or accurate final crack length34 a_{fN} = final crack length determined using the normalization method35 a_{fU} = final crack length determined using the unloading compliance method36 a_{iM} = i^{th} measured or accurate crack length37 a_{iN} = i^{th} calculated crack length by the normalization method38 a_{iU} = i^{th} calculated crack length by the unloading compliance method39 J = J -integral40 J_{Ic} = fracture toughness determined in accordance with ASTM E1820-1841 $J_{Ic(N)}$ = J_{Ic} determined using the normalization method42 $J_{Ic(R)}$ = J_{Ic} determined using the accurate J -R curve method43 $J_{Ic(U)}$ = J_{Ic} determined using the unloading compliance method44 n = strain hardening exponent45 P_i = i^{th} load

7

46 $P_i = i$ th normalized load

47 $S_f =$ the ratio of $(a_{fN} - a_{fM})$ to $(a_{fM} - a_{fU}) = \dot{\iota}$ at final point

48 $S_i =$ the ratio of $(a_{iN} - a_{iM})$ to $(a_{iM} - a_{iU}) = (\dot{\iota} a_{iM} - a_{iN} \vee \dot{\iota}) / (a_{iM} - a_{iU}) \approx S_f$

49 $W =$ specimen width

50 $V_i = i^{\text{th}}$ CMOD

51 $\overline{V}_{pi} = i$ th normalized crack mouth opening displacement

52 **Abbreviations**

53 BT the basic test method

54 CMOD crack mouth opening displacement

55 CT compact tensile specimen

56 J -R J -resistance

57 NM normalization method

58 P - V load-CMOD

59 AJR accurate J -R curve method

60 SE(B) single edge notched specimen

61 UC unloading compliance method

62

63 1. INTRODUCTION

64 Fracture toughness is an important mechanical property of steel used in engineering design
65 and failure assessment of steel structures. In determining the fracture toughness, an essential
66 step is to establish the *J*-Resistance (*J*-R) curves which are usually obtained from laboratory
67 tests. However, tests on *J*-R curves can be difficult because of the difficulties in measuring
68 the crack extension in specimens. There are three methods widely used in these tests, namely
69 the basic test (BT) method, unloading compliance (UC) method and normalization method
70 (NM). In the BT method, the crack extension length is measured physically from the tested
71 specimen, and hence the determined crack extensions can be regarded as accurate. This
72 method requires multiple test specimens to obtain a series of crack extension lengths at each
73 designated level of load ¹⁻³. Obviously, the BT method costs more materials and effort to
74 establish a full *J*-R curve for a material ^{2,3}, but the measurement of crack extension length is
75 considered to be accurate. As such, the BT method has been incorporated in ASTM E1820-18
76 ¹.

77 The unloading compliance (UC) method was first proposed by Clarke et al. ⁴, using elastic
78 properties of the test material to calculate the crack extensions. The UC method has been
79 considered as the most widely used and reliable method for determining the *J*-R curves of
80 materials. It has subsequently been adopted by various standards, such as ASTM E1820 ¹ and
81 BS 7448-4 ⁵. The principle of UC is to relate the crack length to the compliance of the
82 specimen. However, tests with the unloading-reloading processes as required by UC are
83 tedious and time-consuming even with one specimen, compared with the monotonic loading
84 tests. It is also difficult to apply unloading-reloading in harsh conditions, such as high loading
85 rate, high temperature, corrosion, or other aggressive environments. With this regard, the
86 normalization method (NM) was developed by Herrera, Landes ⁶. NM directly uses the

13

87 monotonic load vs. load-line displacement (LLD) or load vs. crack mouth opening
88 displacement (CMOD) record, known as $P-V$ curve, to establish the J -R curve for the
89 specimen without the unloading-reloading process ⁷⁻¹¹.

90 In the normalization method (NM), a calibration function needs to be established to
91 determine the instantaneous crack length corresponding to the load and displacement test
92 data. Various forms of calibration functions have been developed ^{6,7,10,12}. The calibration
93 function adopted in the current standard ASTM E1820-18 Annex 15 ¹ is the four-parameter
94 $LMNO$ (or $a b c d$) function ^{1,12}. NM has since been applied to different materials, including
95 steels ¹²⁻¹⁴, alloys ¹⁵ and polymers ¹⁶⁻²⁰, and structures ²¹.

96 However, J -R curves determined using the unloading compliance (UC) method and the
97 normalization method (NM) are usually different as demonstrated in the literature ²²⁻³⁰. The
98 difference can be quite significant ²⁸⁻³⁰. For example, Dzugan and Viehrig ²² showed that the
99 deviation in fracture toughness resulted from different J -R curves of SFA steel determined by
100 UC and NM was as large as 17%. Zhu and Joyce ²³ found that the deviation in mean fracture
101 toughness of HY80 steel using UC and NM was around 11%. For HSLA steel, the deviation
102 in mean fracture toughness J_{Ic} using UC and NM was found to be 9% by Menezes et al. ²⁷.
103 Moreover, the average difference in J_{Ic} of G250 steel using UC and NM can be as large as
104 26% ²⁸. It is reasonable to infer that one or both of these two methods cannot determine the J -
105 R curves of tested specimens accurately when the difference is large. As both UC and NM
106 are incorporated in ASTM E1820, which is the most commonly used standard, the difference
107 in the J -R curves using these two methods may cause confusion and issues in engineering
108 practice. Therefore, there is a genuine need to develop a new method that can determine the
109 J -R curve accurately.

14 5

15

110 As it is known, J -R curves are derived from P - V curves which are raw load and displacement
111 records and hence should be the same for all methods used. Results from the tests with
112 different specimens and materials conducted by Gao et al ²⁸⁻³⁰ proved that, for an arbitrary
113 point on the P - V curve, the J -integral determined by UC and NM is almost the same ²⁸.
114 Wallin and Larkkanen ³¹ also proved that the J -integral calculated in the basic test (BT)
115 method is identical to the J -integral calculated using the single-specimen test, such as UC.
116 Fortes and Bastian ³² further found that the J -integral calculated using the BT method and
117 NM is nearly the same (<4%). Therefore, all the three methods, i.e., BT, UC and NM, can
118 determine the same J -integral accurately.

119 However, these three methods produce different crack (extension) lengths for given J
120 measurements, leading to different J -R curves. Clearly, the inaccurate estimation of crack
121 (extension) length is the root cause of the problem in determining J -R curves. For the basic
122 test (BT) method, the crack (extension) lengths are measured physically and theoretically is
123 more accurate. For the unloading compliance (UC) method, the estimated crack (extension)
124 length is underestimated, whilst for the normalization method (NM) the estimated crack
125 (extension) length is overestimated as previously proved in Gao et al ^{29,30}. Intuitively, if there
126 is a method that can determine the crack (extension) length accurately, an accurate J -R curve
127 can be determined and so is the fracture toughness. Based on this idea, this paper aims to
128 develop a new method that can determine the crack (extension) length accurately, leading to
129 an accurate J -R curve and fracture toughness. The new method is developed based on the
130 experimental observation and analytical derivation, and hereafter is referred to as the accurate
131 J -R curve method, denoted as AJR method. Factors that demonstrate the significance of the
132 newly developed AJR method are also investigated.

133 The merit of the developed new AJR method is that it combines the advantages of the
134 accuracy of BT, the popularity of UC and the simplicity of NM. The new AJR method can
135 contribute to the body of knowledge of fracture mechanics by determining an accurate J -R
136 curve and then fracture toughness. This is one of the most challenging issues in fracture
137 mechanics at the present but nevertheless is its fundamental objective. The new AJR method
138 and its results presented in this paper can assist engineers and researchers to determine the
139 accurate J -R curves and fracture toughness of steels, which fills the gap in current fracture
140 mechanics as demonstrated in the literature survey (see References). Accurate determination
141 of fracture toughness can effectively prevent structural failures due to the overestimation of
142 the fracture toughness and can also effectively reduce the cost of materials due to the
143 underestimation of the fracture toughness.

144 **2. DEVELOPMENT OF NEW METHOD**

145 **2.1 Experimental Observation**

146 In the basic test (BT) method, identical multiple specimens are used to determine the J -R
147 curve of materials. Each of the (presumed) identical specimens is loaded to a designated level
148 of load to produce a P - V curve at that level and then unloaded for the measurement of the
149 crack extension. The corresponding J -integral value is calculated from the P - V curve for each
150 specimen to create a point on the J -R curve for the test material. In BT, each specimen
151 actually produces one intermediate point on the J -R curve for the tested material. Together
152 with the multiple specimens, a full J -R curve can be produced for the tested material in the
153 same way as if it were produced from one specimen. It is well known that the crack
154 (extension) length determined by BT is more accurate as it is physically measured. Test
155 results have proved that the P - V and J -R curves of nearly identical specimens are almost the
156 same^{27,28,33,34}. There is a one-to-one corresponding relationship between the point on the P - V

157 curve and that on the J -R curve in terms of loading P and J -integral. The final points on the
 158 J -R curves, i.e., J -integral vs. crack extension of the tested multiple specimens at different
 159 levels of loading can be regarded as the intermediate points on the J -R curve of a single
 160 specimen.

161 Table 1 presents results from the tests by Gao et al. ²⁸⁻³⁰ for three types of steel with six 10
 162 mm CT specimens, six 10 mm SE(B) specimens and six 16 mm SE(B) specimens. It shows
 163 the final crack lengths determined by the actual measurement on the fracture surface, the
 164 unloading compliance (UC) method and the normalization method (NM), respectively. These
 165 three differently determined final crack lengths correspond to the same final point on the P - V
 166 curve of the specimen. The calculated J -integral value of this final point using the three
 167 methods is the same, but the crack (extension) lengths are different. Then, for a given final
 168 point $f(P_f, V_f)$ on the P - V curve of a specimen, let the differences between the measured
 169 crack length and the one determined by UC and NM be $a_{fM} - a_{fU}$ and $a_{fM} - a_{fN}$, respectively.
 170 Now define the ratio of these differences as follows

$$171 \quad S_f = \frac{a_{fM} - a_{fU}}{a_{fM} - a_{fN}} \quad (1)$$

172 since $a_f = a_0 + \Delta a_f$

$$173 \quad S_f = \frac{\Delta a_{fU}}{\Delta a_{fN}} \quad (2)$$

174 S_f is referred to as the ratio of final crack length differences. From the test results on the final
 175 crack length determined by different methods as shown in Table 1, it can be seen clearly that
 176 S_f for all specimens tested in a group (as duplicates or identical specimens) are almost the
 177 same. For example, two identical specimens tested in the group G350-C-10 are G350-C-10-

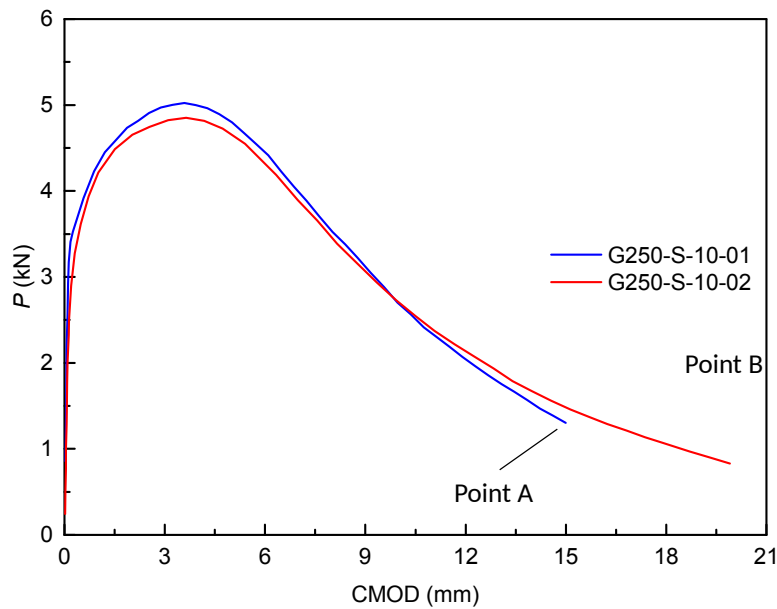
178 01 and G350-C-10-02 with the same S_f of 0.362 (see 3rd and 4th rows from the bottom of
179 Table 1).

180 Table 1 Final crack lengths determined from different methods

Material	Configuration	Thickness (mm)	Specimen No.	UC a_{fU} (mm)	Measured a_{fM} (mm)	NM a_{fN} (mm)	S_f
Weldox700	SE(B)	16	W700-S-16-01	25.03	26.37	27.74	1.022
Weldox700	SE(B)	16	W700-S-16-02	25.13	26.36	27.68	1.073
G350	SE(B)	16	G350-S-16-01	27.23	29.07	29.65	0.315
G350	SE(B)	16	G350-S-16-02	25.16	27.19	27.80	0.300
G250	SE(B)	16	G250-S-16-01	25.35	25.97	27.11	1.839
G250	SE(B)	16	G250-S-16-02	22.42	23.53	25.53	1.802
Weldox700	SE(B)	10	W700-S-10-01	16.87	17.67	18.05	0.475
Weldox700	SE(B)	10	W700-S-10-02	17.12	18.24	18.78	0.482
G350	SE(B)	10	G350-S-10-01	17.81	18.44	19.16	1.143
G350	SE(B)	10	G350-S-10-02	17.9	18.57	19.36	1.179
G250	SE(B)	10	G250-S-10-01	16.14	16.96	17.35	0.476
G250	SE(B)	10	G250-S-10-02	16.62	17.56	18.00	0.468
Weldox700	CT	10	W700-C-10-01	25.3	26.24	26.56	0.340
Weldox700	CT	10	W700-C-10-02	28.41	29.93	30.45	0.342
G350	CT	10	G350-C-10-01	32.36	34.1	34.73	0.362
G350	CT	10	G350-C-10-02	36.02	37.4	37.90	0.362
G250	CT	10	G250-C-10-01	28.04	29.88	30.47	0.321
G250	CT	10	G250-C-10-02	31.43	33.78	34.55	0.328

181 Let the final points of two arbitrarily selected identical specimens be Point A and B on the P -
182 V curve of the tested material. Taking specimens G250-S-10-01 and 02 from Gao et al.²⁸ as
183 an example, the P - V curves of these two specimens are shown in Fig. 1. It can be seen that
184 the P - V curves are nearly identical for these two specimens, even the tests are stopped at the
185 different levels of loading. The J - R curves of these two specimens are also nearly identical as
186 shown in Gao et al.²⁸. The P - V curve of G250-S-10-01 can be regarded as a part of the P - V
187 curve of G250-S-10-02, as in the basic test method where multiple specimens are required.
188 Point A is an intermediate point corresponding to a specific level of loading on this P - V curve
189 of G250-S-10-02. Point A can be regarded as an arbitrary point (P_b , V_b) on the P - V curve and
190 Point B is the final point. The location of Point A depends on the level of loading at which
191 the test stops. It can be seen from Table 1 that the ratios of final crack length differences

192 corresponding to Point A and B are the same (see 3rd and 4th rows from the bottom of Table
 193 1). Therefore, for an arbitrary point i (P_i , V_i) on the P - V curve, its corresponding crack
 194 length difference ratio (S_i) is the same as that of the final point of the P - V curve, i.e., S_f .
 195 Further examination of the results in Table 1 can show that the crack length difference ratios
 196 at any two points are all the same for all other groups in Table 1. This is an important
 197 discovery that reveals the consistency of crack length difference ratios at any point of the P - V
 198 curve of a specimen. It is referred to as crack length difference compliance and measured by
 199 a crack length difference ratio S_i .



200

201

Figure 1 P - V curves of G250-S-10-01 and 02

202 Thus, for a given point i (P_i , V_i), let the differences between the measured crack length and
 203 the one determined using UC and NM be $a_{iM} - a_{iU}$ and $a_{iM} - a_{iN}$, respectively. Then the ratio
 204 of these two differences is as follows

$$205 \quad S_i = \frac{a_{iM} - a_{iU}}{a_{iM} - a_{iN}} \approx S_f \quad (3)$$

31

206 Equation (3) is the mathematical expression of the principle of crack length difference
 207 compliance which is the basis for the new method to be developed.

208 **2.2 Analytical Derivation**

209 It has been proved above that for an arbitrary point (P_i, V_i) on the $P-V$ curve, the
 210 corresponding crack length difference ratio S_i is equal to S_f , which can be determined by each
 211 or all of the basic test (BT) method, unloading compliance (UC) method and normalization
 212 method (NM). Thus, an accurate or measured crack length a_{iM} corresponding to this point
 213 can be determined from Equation (3) as follows

$$214 \quad a_{iM} = (a_{iN} + S_i a_{iU}) / (S_i + 1) = (a_{iN} + S_f a_{iU}) / (S_f + 1)$$

215 (4)

216 where a_{iN} and a_{iU} can be determined using NM and UC, respectively at the point (P_i, V_i) , S_i
 217 $\approx S_f$, and S_f can be determined with Equation (1) using the final point of the $P-V$ curve.

218 With an accurate crack length a_{iM} known, the crack extension Δa_{iM} can be determined
 219 accurately, i.e., $\Delta a_3 = a_3 - a_0$. Also, it can be recalled that the J -integral is the same as that
 220 determined by all three methods (i.e., BT, UC and NM), and the determined J is regarded as
 221 accurate. Therefore, an accurate J -R curve can be established. Since the developed new
 222 method primarily aims to determine the accurate J -R curve, it is referred to as the accurate J -
 223 R curve method, donated as AJR.

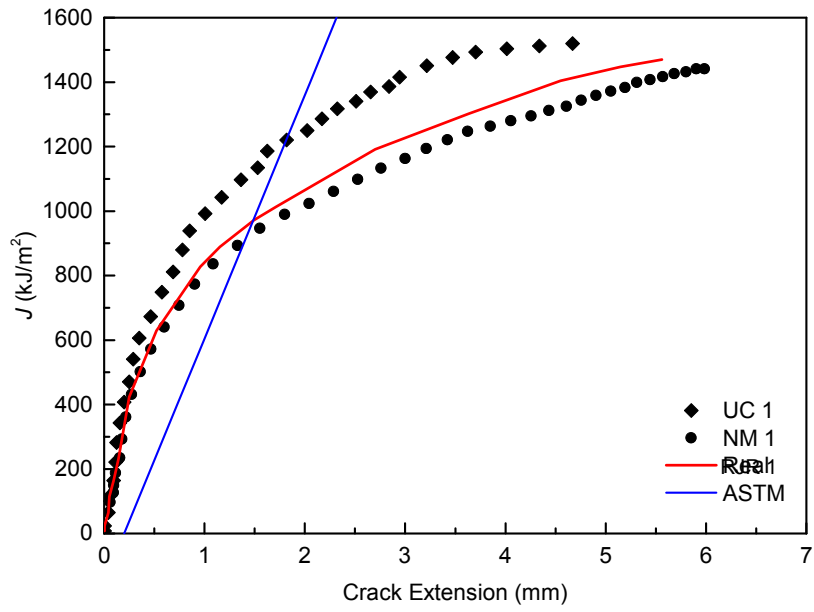
224 **2.3 Procedure for New Method**

225 As stated above, the developed AJR method aims to accurately determine the crack
 226 (extension) length corresponding to a point on the $P-V$ curve. This can be achieved by

227 measuring the final crack (extension) length of a tested specimen. The J -integral can be
 228 determined using UC and NM for the specimen. Therefore, the J -R curve for the test material
 229 can be determined accurately. The procedure for determining the accurate J -R curve for a
 230 specimen using the developed AJR method is as follows.

- 231 1. Obtain the P - V curve for the specimen with unloading-reloading processes.
- 232 2. Measure the initial and final crack lengths of the tested specimen, i.e., a_0 and a_f .
- 233 3. Determine the crack extension lengths and J -integrals of this specimen using UC and
 234 NM, respectively.
- 235 4. Calculate the final crack lengths, a_{fU} and a_{fN} , using UC and NM, respectively.
- 236 5. Calculate the final crack length difference ratio S_f for the final point on the P - V curve of
 237 the specimen, using Equation (1).
- 238 6. Calculate the accurate crack length at an arbitrary point i on the P - V curve, a_{iM} , using
 239 Equation (4), and the accurate crack extension length ($\Delta a_3 = a_3 - a_0$).
- 240 7. Determine the J -integral value corresponding to the i point on the P - V curve, i.e., J_i , from
 241 step 3.
- 242 8. For different points ($J_i, \Delta a_{iM}$), determined from steps 7 and 6, an accurate J -R curve can
 243 be established.

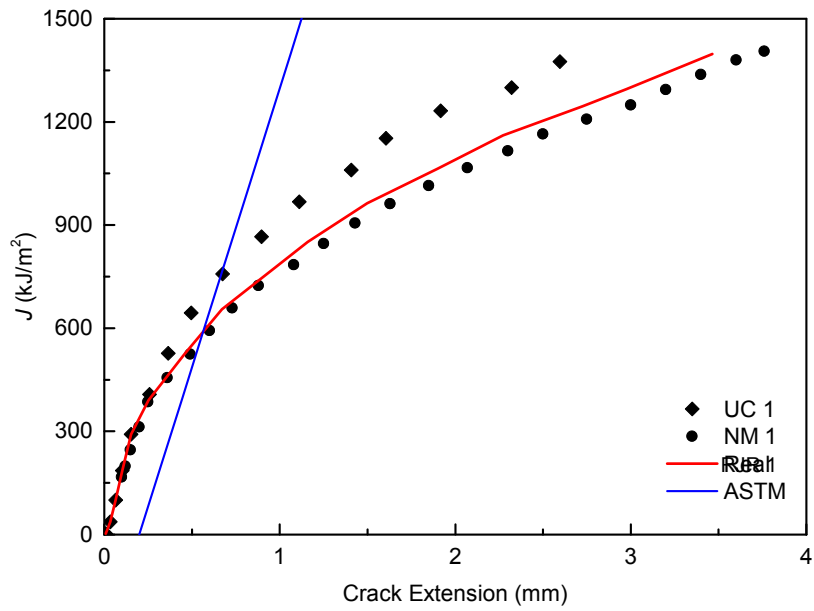
244 Based on this procedure, a number of examples were given to accurately establish the J -R
 245 curves using data taken from Gao et al.²⁸⁻³⁰ as presented in Table 1. The results of the J -R
 246 curves determined by AJR are shown in Fig. 2, together with those from the unloading
 247 compliance (UC) method and normalization method (NM). It can be seen that the accurately
 248 determined J -R curves are in between those determined by UC and NM, clearly reflecting the
 249 underestimation of J_{Ic} by NM and the overestimation of J_{Ic} by UC consistently as stated in
 250 Section 1.



251

252

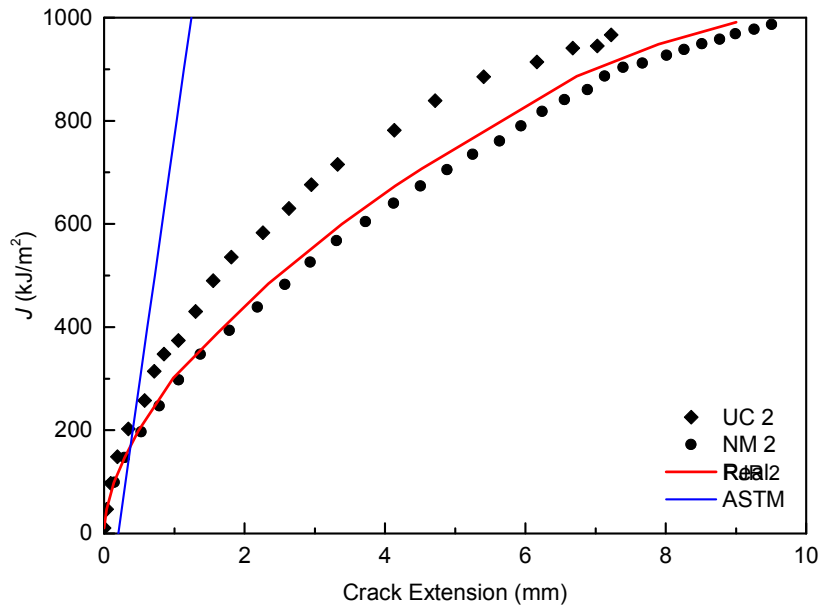
(a)



253

254

(b)



255

256

(c)

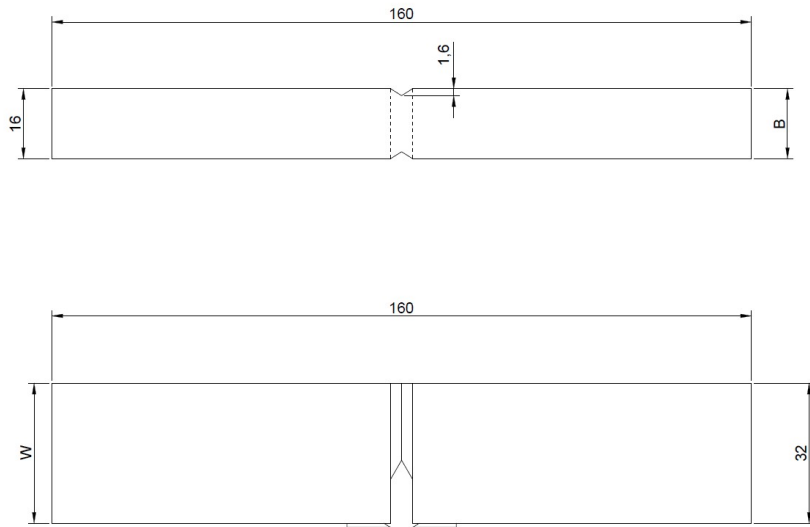
257 Figure 2 Accurate J - R curve and fracture toughness of specimens: (a) G250-S-10-01; (b)
 258 W700-C-10-01; (c) G350-S-16-02

259

260 3. EXPERIMENTAL VERIFICATION

261 3.1 Test Specimen and Method

262 To verify the developed new AJR method, two series of new tests were carried out with
 263 different steels for the J - R curves and fracture toughness. Three types of Australian steel
 264 were used: Wieldox700, G350 and G250. The mechanical properties of these three types of
 265 steel are taken from Gao et al. ²⁸. There are two specimens for each steel with a total of 6
 266 SE(B) specimens. The dimensions of the specimens are 160 mm in length, 32 mm in width
 267 and 16 mm in thickness. All specimens are side grooved to the thickness reduction of 20%.
 268 The configuration of the specimens is shown in Fig. 3.

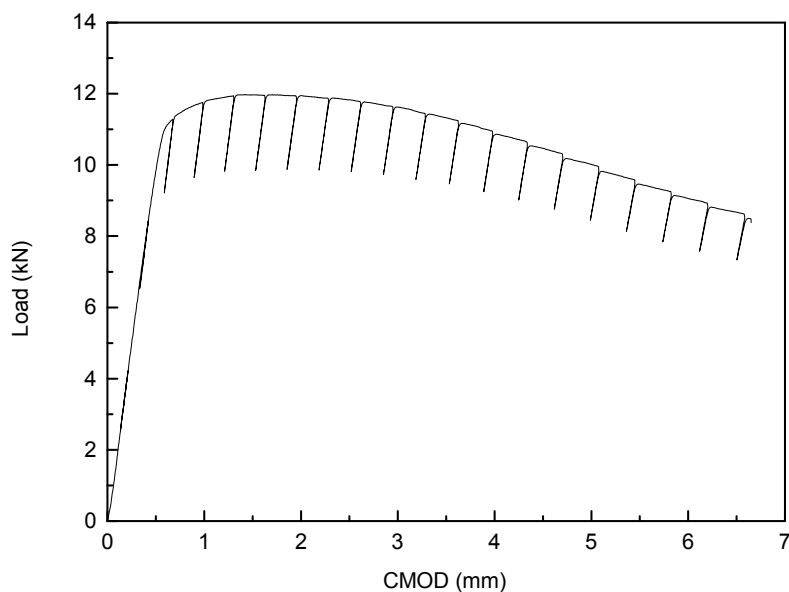


269

270

Figure 3 Configuration of tested SE(B) specimen

271 Two SE(B) specimens were tested for each type of steel. All tests were carried out under the
 272 quasi-static loading condition and room temperature. As an example, the obtained load-
 273 CMOD curve for specimen W700-S-16-03 with unloading-reloading cycles is shown in Fig.
 274 4. The load-CMOD curves of other specimens are in a similar form and thus are not repeated
 275 here. The data for the normalization method is taken from the envelope curves of the
 276 unloading compliance experiments.

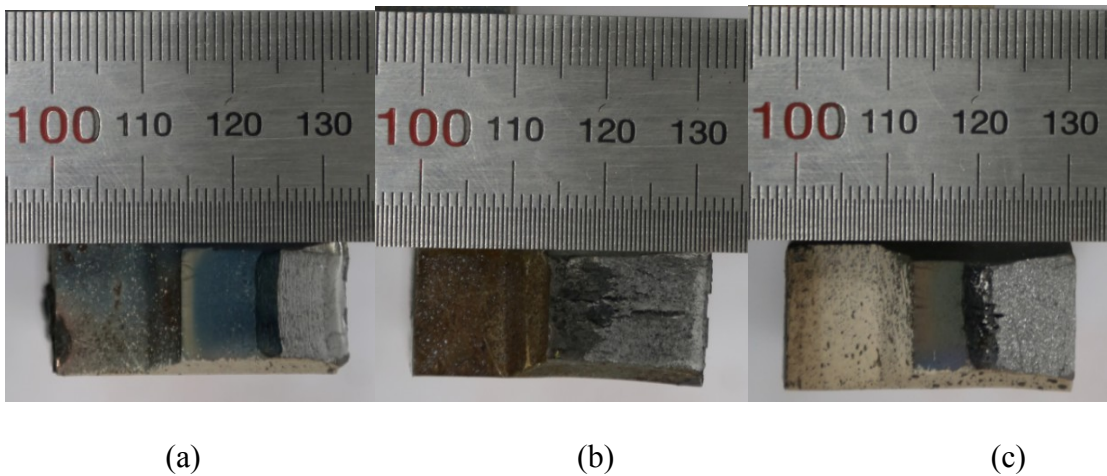


277

278

Figure 4 Load vs CMOD curve of specimen W700-S-16-03

279 After the tests, all specimens were heat tinted under 300°C for 30 minutes, then refrigerated,
 280 and broken following ASTM E1820 ¹. The final crack lengths of specimens were measured
 281 by a digital imaging tool following the nine-point average method recommended in ASTM
 282 E1820 ¹ and BS 7448-4 ⁵, and are shown in Table 2. Fig. 5 illustrates the typical fracture
 283 surfaces for different types of steel. The plane strain condition for crack growth was
 284 confirmed for Weldox700 and G250 steel as the nearly straight lines were found along the
 285 crack front at the crack tips for the tested specimens ^{2,35}. For G350 steel, slightly inclined
 286 crack fronts at the crack tip do not affect achieving the plane strain condition, as 16 mm
 287 thickness was proved to be sufficiently thick for plane strain condition ^{28,29}. The slightly
 288 inclined crack fronts at the crack tip for specimens G350-S-16-03 and 04 are because of the
 289 non-pre-cracking. The effect of pre-cracking will be discussed in Section 4.3.



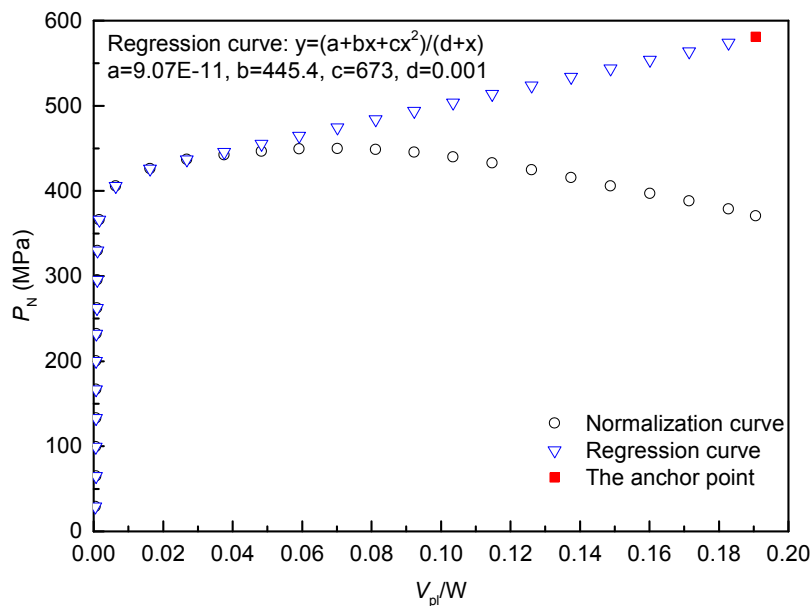
292 Figure 5 Fracture surfaces of specimens: (a) Weldox700, (b) G350, (c) G250 (major unit 10
 293 mm)

294 Table 2 Newly tested specimens and their final crack lengths

Material	Configuration	Thickness (mm)	Specimen No.	UC a_{fU} (mm)	Measured a_{fM} (mm)	NM a_{fN} (mm)	S_f
Weldox700	SE(B)	16	W700-S-16-03	24.43	25.02	25.61	1.000
Weldox700	SE(B)	16	W700-S-16-04	24.78	25.3	25.86	1.077
G250	SE(B)	16	G350-S-16-03	22.44	23.03	24.08	1.780
G250	SE(B)	16	G350-S-16-04	25.77	26.39	27.49	1.774
G350	SE(B)	16	G250-S-16-03	20.37	20.82	21.93	2.467
G350	SE(B)	16	G250-S-16-04	21.56	22.02	23.15	2.457

295 3.2 Determination of J -R Curves

296 The normalized load vs normalized plastic CMOD curves are obtained from the load-CMOD
 297 (P - V) records. Fig. 6 shows the typical normalized load vs normalized plastic CMOD curves
 298 obtained via the normalization method (NM) for W700-S-16-03 as an example, where P_i is
 299 the i^{th} normalized load, and V_{pl} is the plastic part of CMOD. For specimens of W700-S-16-04
 300 and other steels, similar curves are obtained and thus are not repeated. The final crack length
 301 is physically measured from the fracture surface and is used with the final load to develop the
 302 anchor point. Subsequently, regression is used to determine the coefficients a , b , c and d
 303 according to Equation A15.5 in ASTM E1820 A15¹.

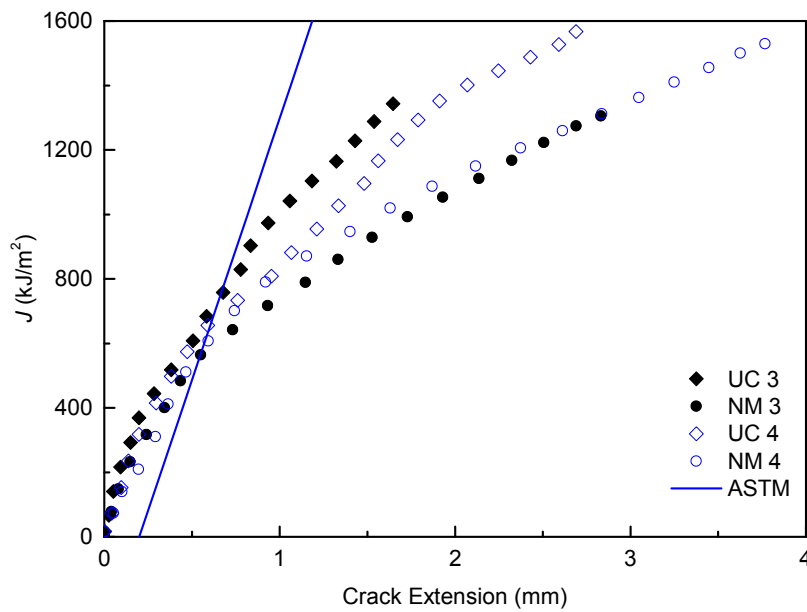


304

305 Figure 6 Normalized load vs normalized plastic CMOD for specimen W700-S-16-03

306 With a , b , c , and d determined, an iterative procedure is used to determine the a_i value for each
 307 P_i , and then J -integral values for each P_i are calculated. Finally, the J -R curves of all
 308 specimens tested in this study are obtained via the unloading compliance (UC) method and
 309 the normalization method (NM), as shown in Fig. 7. ‘UC 3’ and ‘NM 3’ in these figures
 310 represent the J -R curve obtained using UC and NM from specimens 03, respectively, while
 311 ‘UC 4’ and ‘NM 4’ are from the specimens 04. The straight lines, used in the current work,

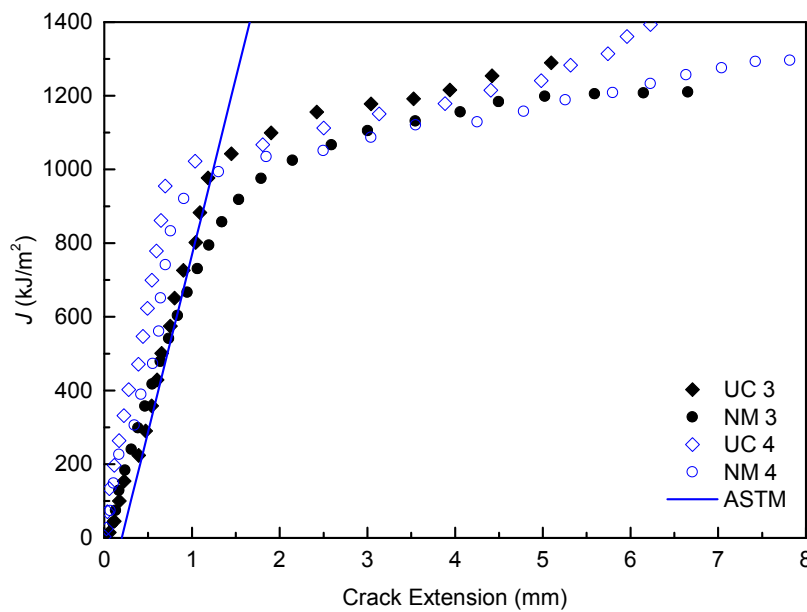
312 are 0.2 mm offset lines recommended by ASTM E1820 ¹. Table 2 illustrates the final crack
 313 lengths determined by measurement, UC and NM for the tested specimens. For G350 16 mm
 314 specimens, it can be seen from Tables 1 and 2 that the pre-cracked specimens G350-S-16-01
 315 and 02 have the same S_f value, while the non-pre-cracked specimens G350-S-16-03 and 04
 316 also have the same S_f value. This explains further the compliance of crack length difference
 317 which is not affected by the processing of specimens.



318

319

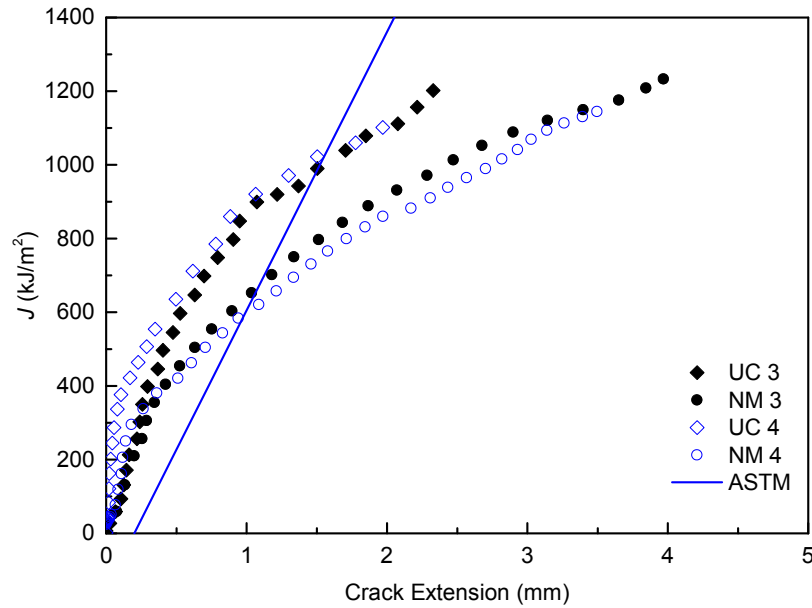
(a)



320

321

(b)



(c)

322

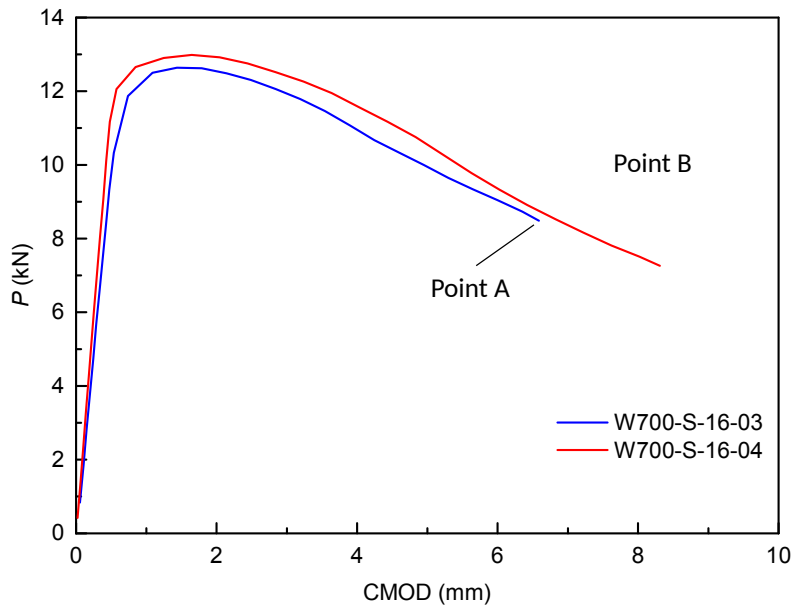
323

324 Figure 7 J - R curves of steels using unloading compliance and normalization method: (a)
 325 Weldox700 steel; (b) G350 steel; (c) G250 steel

326 3.3 Verification of the New Method

327 To verify the developed accurate J - R curve (AJR) method, newly tested Weldox700
 328 specimens are used as examples, the results of which are presented in Table 2. The tested P - V
 329 curves of these two specimens are shown in Fig. 8. It can be seen that the P - V curves are
 330 nearly identical for these two specimens, even the tests are stopped at different levels of
 331 loading. The J - R curves determined using NM of these two specimens are nearly identical as
 332 shown in Fig. 7 (a). As explained in Section 3.1, the P - V curve of W700-S-16-03 can be
 333 regarded as a part of the P - V curve of W700-S-16-04, and Points A and B are two different
 334 points corresponding to different loading levels on the P - V curve of W700-S-16-04. Point A
 335 can be regarded as an arbitrary point (P_i, V_i) on the P - V curve of W700-S-16-04 and Point B
 336 is the final point. The corresponding S_i values of Points A and B are the same that can be seen
 337 from the 2nd and 3rd rows in Table 2. Moreover, Table 1 shows the S_i values of W700-S-16-01
 338 and W700-S-16-02 from which it can be seen that the S_i values of all these four Weldox700
 339 specimens are almost the same. Thus, for an arbitrary point i (P_i, V_i) on the P - V curve, its

340 corresponding crack length difference ratio S_i is the same as that of the final point, i.e., S_f , on
 341 the $P-V$ curve. Therefore, the principle of crack length difference compliance, as expressed in
 342 $S_i \approx S_f$, is proved. This S_i consistency also can be found in other newly test specimens as
 343 shown in Table 2.

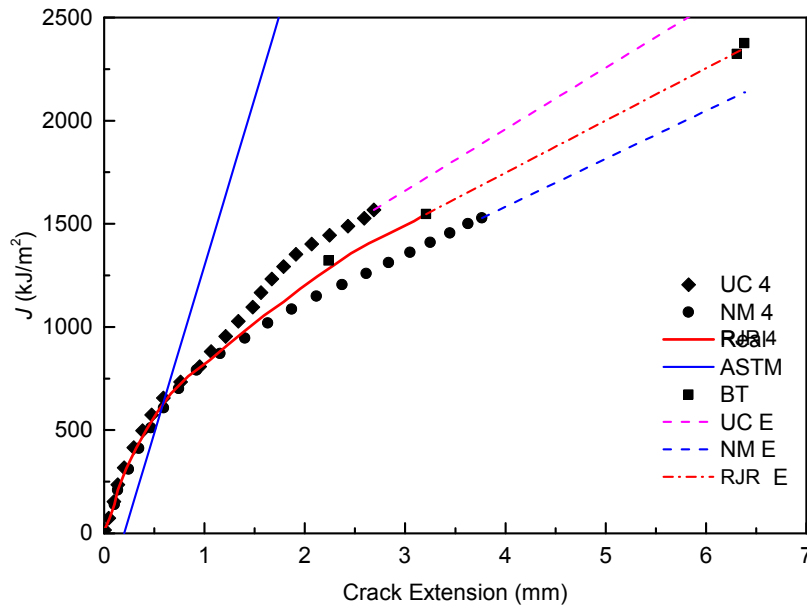


344

345 Figure 8 $P-V$ curves of specimens W700-S-16-03 and 04

346 After the compliance principle is proved, the accurate crack length or crack extension length
 347 corresponding to any point on the $P-V$ curve can be determined using Equation (4). Then the
 348 accurate $J-R$ curves of the specimens can be determined following the procedures of AJR
 349 outlined in Section 2.3. The $J-R$ curves determined using the basic test (BT) method can be
 350 obtained with the data produced from specimens tested in this study and supplementary data
 351 from Table 1. For instance, the specimens W700-S-16-01 to 04 can be used to obtain the $J-R$
 352 curve using BT. Fig. 9 shows the accurate $J-R$ curve determined using AJR compared with
 353 those determined using other methods, i.e., BT, UC and NM, for the newly tested specimens.
 354 In Fig. 9, specimens 04 are used as its crack lengths are longer than those of 03. The dash
 355 lines are the extended lines of $J-R$ curves determined by UC, NM and AJR, as the final crack
 356 extension lengths for W700-S-16-01 and G250-S-16-01 are longer than those of the newly

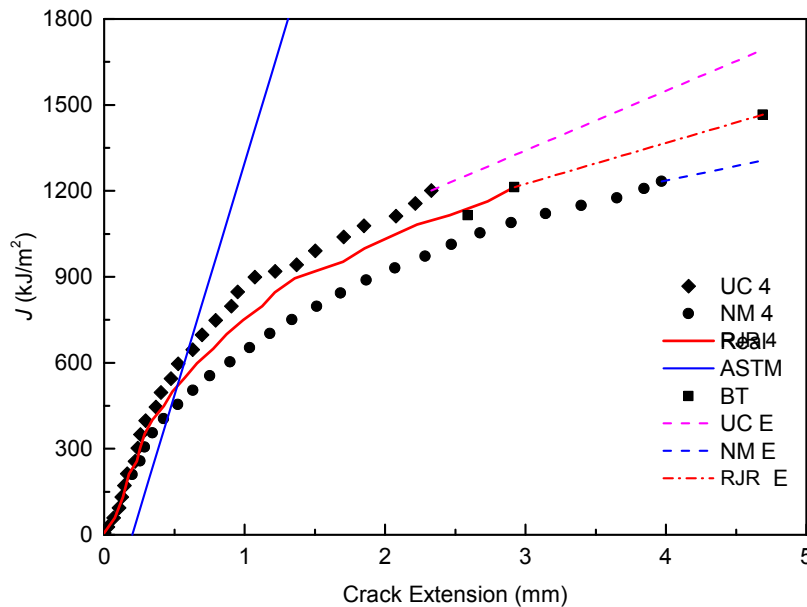
357 tested specimens. It can be seen clearly that the J -R curve determined by AJR is the closest to
 358 that by the BT method. As the J -R curves determined by the basic test (BT) method is
 359 considered to be accurate because of the accurate measurement of crack (extension) length,
 360 i.e., a benchmark, the developed accurate J -R curve method, AJR, is verified.



361

362

(a)



363

364

(b)

365 Figure 9 J -R curves of specimens determined by different methods: (a) W700-S-16-04; (b)
 366 G250-S-16-04

367 It may be noted that the J -R curve obtained from multiple specimens cannot completely
368 coincide with the accurate J -R curve of a single specimen, as shown in Fig. 9. This is because
369 there are many factors in the testing that are difficult to control accurately. For example, the
370 material of the specimens may not be completely uniform, and the fatigue pre-cracked length
371 is difficult to control. Thus, the difficulty to obtain completely identical J -R curves is
372 understandable and this difficulty actually endorses that the accurate J -R curve determined
373 using AJR is more appropriate than that determined using the BT method. Moreover, the BT
374 method requires multiple specimens, which is wasteful and is one of the main reasons to
375 develop the single-specimen test methods, such as UC and NM, but UC and NM are not as
376 accurate as the developed AJR. This again vindicates the need to develop an accurate single-
377 specimen test method for determining the accurate J -R curve, as it is developed, i.e., AJR, in
378 this paper.

379 4. DISCUSSION AND FURTHER ANALYSIS

380 4.1 Fracture Toughness

381 As it is known, it is the fracture toughness of steel that is used in engineering design and
382 assessment of steel structures. Thus, the significance of the developed new AJR method is
383 that it can determine the accurate, i.e., the accurate fracture toughness based on the accurate
384 J -R curves. Table 3 gives the accurate fracture toughness determined for every specimen
385 shown in Table 1 following ASTM E1820. Two specimens of Weldox700 SE(B) 10 mm are
386 not included because relatively close J -R curves were determined using the unloading
387 compliance (UC) method and normalization method (NM). The accurate fracture toughness
388 of the newly tested specimens is shown in Table 4.

389 Table 3 Accurate fracture toughness of specimens from existing tests

Specimen		ASTM E1820-18 (J_{Ic} ; kJ/m ²)						
		Deviation (%)		UC $J_{Ic(U)}$;	Accurate $J_{Ic(A)}$;	NM $J_{Ic(N)}$;	Deviation (%)	
SE(B) 16mm	Weldox700 01	10.29	6.87	699	651	604	7.22	5.72
	Weldox700 02		13.72	605	522	500	4.21	
	G350 01	17.84	13.00	223	194	186	4.12	3.79
	G350 02		22.67	225	174	168	3.45	
	G250 01	11.33	8.26	1138	1044	886	15.13	21.16
	G250 02		14.40	1680	1438	1047	27.19	
SE(B) 10mm	G350 01	6.96	6.94	216	201	169	15.92	12.96
	G350 02		6.98	215	200	180	10.00	
	G250 01	13.86	20.26	1219	972	903	7.10	13.32
	G250 02		7.46	1233	1141	918	19.54	
CT 10mm	Weldox700 01	17.84	19.02	736	596	574	3.69	3.60
	Weldox700 02		16.67	546	455	439	3.52	
	G350 01	20.28	23.53	136	104	97	6.73	6.94
	G350 02		17.04	135	112	104	7.14	
	G250 01	30.40	30.16	809	565	532	5.84	5.30
	G250 02		30.64	607	421	401	4.75	

390

391

Table 4 Accurate fracture toughness of the newly tested specimens

Specimen		ASTM E1820-18 (J_{Ic} ; kJ/m ²)						
		Deviation (%)		UC $J_{Ic(U)}$;	Accurate $J_{Ic(A)}$;	NM $J_{Ic(N)}$;	Deviation (%)	
SE(B) 16mm	Weldox700 03	12.69	18.16	727	595	564	5.21	4.71
	Weldox700 04		7.22	665	617	591	4.21	
	G350 03	6.94	9.48	802	726	603	16.94	10.92
	G350 04		4.40	1046	1000	951	4.90	
	G250 03	12.54	9.80	990	893	662	25.87	28.92
	G250 04		15.27	1041	882	600	31.97	

392

393 It can be seen from Tables 3 and 4 that the differences between the accurate fracture
394 toughness ($J_{Ic(A)}$) and that determined using UC ($J_{Ic(U)}$) or NM ($J_{Ic(N)}$) for the given specimen
395 are all larger than 10%. For example, the difference between J_{Ic} determined using the three
396 methods (AJR, UC, NM) are larger than 10% for G250 SE(B) specimens, which clearly
397 shows the significance of the developed new AJR method; otherwise, inaccurate fracture

398 toughness determined using UC or NM, i.e., $J_{Ic(U)}$ or $J_{Ic(N)}$ can lead to failures of steel or steel
 399 structures. Therefore, the developed new AJR method is especially necessary to determine
 400 the accurate fracture toughness for G250 specimens. For all other specimens listed in Table 3
 401 and 4, it also can be found that the AJR method is necessary to determine the fracture
 402 toughness, i.e., $J_{Ic(A)}$ because the difference between $J_{Ic(U)}$ and $J_{Ic(A)}$, and/or $J_{Ic(N)}$ and $J_{Ic(A)}$ are
 403 all larger than 10%.

404 4.2 Effect of Mechanical Properties

405 The inaccuracy in determining the J - R curves using the unloading compliance (UC) method
 406 and normalization method (NM) essentially lies in the difference in determining the crack
 407 lengths. This difference or disagreement is influenced by the mechanical properties of the
 408 steel. The larger this disagreement is the more inaccurate the J - R curves are and hence the
 409 more necessary the developed new AJR method is. Therefore, it is of more importance to
 410 apply the AJR method to those steels with the mechanical properties that incur the largest
 411 disagreement in the J - R curves between UC and NM.

412 Based on test results from three types of steel in ²⁸ it can be found that the difference in J - R
 413 curves and fracture toughness determined using UC and NM is larger for materials with
 414 lower strain hardening ratio and effective yield strength ^{28,30}, such as G250 steel (also see
 415 Section 4.1 above). For example, for given specimen configuration and thickness, it can be
 416 seen from Table 5 ²⁸ that the average difference in tested J_{Ic} is only 8.93% for W700-S-10-01
 417 and 02, while the average difference in J_{Ic} is 25.74% for G250-S-10-01 and 02, which proves
 418 that it is more appropriate to employ the developed new AJR method in determining the
 419 fracture toughness for steels with lower strain hardening ratio and effective yield strength.

420 Table 5 Fracture toughness of three types of steel ²⁸

	ASTM E1820-18 (J_{Ic} ; kJ/m ²)
--	--

G350-S-10-02	215	180	16.3	25.7
G250-S-10-01	1219	903	25.9	
G250-S-10-02	1233	918	25.5	

421

422 4.3 Effect of Specimen Geometry and Configuration

423 The accuracy of the developed new AJR method should not be affected by the geometry and
 424 configuration of the specimens due to the principle of crack length difference compliance.
 425 However, the geometry and configuration of the specimen do affect the disagreement
 426 between UC and NM. Thus, identifying the geometries and configurations that cause the
 427 largest difference would help users to choose the newly developed AJR method.

428 It has been proved theoretically and experimentally in ³⁰ that the thicker specimen, lower
 429 initial crack length to width (a_0/W) and CT configuration result in a larger difference in J -R
 430 curves and fracture toughness between UC and NM. For instance, the average difference in
 431 the tested J_{Ic} between W700-S-10-01 and 02 is only 8.93%, but the average difference in the
 432 tested J_{Ic} between W700-S-16 specimens and W700-C-10 is over 18.14% ²⁸⁻³⁰. Clearly, the
 433 geometry and configuration play a significant role in UC and NM methods. Gao et al. ³⁰ also
 434 found that the largest disagreement between UC and NM is from thicker CT specimens with
 435 shallower initial crack length. Thus, the developed AJR method should be the first choice for
 436 specimens with these geometries and configurations.

437 The effect of non-pre-cracking on the disagreement between UC and NM has not been
 438 investigated in the published literature. For G350 steel, specimens G350-S-16-01 and 02 were
 439 pre-cracked ²⁹, while the specimens G350-S-16-03 and 04 were not pre-cracked. The radius
 440 of the crack tip in the specimen G350-S-16-03 and 04 is designed to be 0.5 mm. The
 441 difference in specimens is only the pre-cracking. From Tables 3 and 4 it can be found that
 442 non-pre-cracking influences the value of tested fracture toughness. The average tested

443 fracture toughness of G350 03 and 04 is around 5 times of that of G350 01 and 02, which is
444 very large. Joyce and Gudas ³⁶ produced the same test results. However, the difference in J_{Ic}
445 determined using UC and NM is almost the same for pre-cracked and non-pre-cracked G350
446 specimens. Therefore, whilst the pre-cracking influences the tested fracture toughness
447 considerably, the method used does not, which means the disagreement in the tested fracture
448 toughness between UC and NM is negligible. As such the developed new AJR has little
449 advantage for specimens with or without pre-cracking.

450 **4.4 Effect of Final Crack Extension Length**

451 Dzugan and Viehrig ²² observed from their test results that exceeding the crack extension
452 length limit prescribed in ASTM E1820-18 A15 ¹ did not cause extensive errors for CT and
453 SE(B) specimens by NM. Gao et al. ³⁰ also found that the disagreement between UC and NM
454 was not influenced by the final crack extension. Gao et al. ³⁰ conducted the tests on 10mm CT
455 specimens to investigate the influence of crack extension. Specimens No.1 with three types of
456 steel were tested following the crack extension limit of ASTM E1820-18 A15 ¹, while the
457 specimens No.2 were not. It was found in Gao et al. ³⁰ that the disagreement between UC and
458 NM was almost the same (<5%) for 10mm CT specimens 01 and 02 of all three tested steels.
459 Therefore, as the disagreement between UC and NM is almost the same for specimens with
460 different final crack extension lengths, the advantage of the developed new AJR method is
461 not obvious for specimens with and without the final crack extension limit.

462 It is worth acknowledging that one important factor that affects the fracture toughness is the
463 standard used. But standards do not affect the J - R curve and as such will not be discussed
464 here. Also, standards are regulatory issues, albeit based on technical evidence, which are
465 better to leave it out of the scope of this paper.

466 **5. CONCLUSION**

467 Considerable difference in J -R curves determined by unloading compliance (UC) method and
468 normalization method (NM) has motivated researchers to develop a new accurate method. In
469 this paper, the crack length difference compliance as measured by the crack length difference
470 ratio S_i has been discovered, analysed and then verified by experiments. Based on the
471 principle of crack length difference compliance, a new accurate method, known as AJR, has
472 been developed. To verify the developed AJR method, new tests on different steels with
473 different specimen configurations have been undertaken. Factors that demonstrate the
474 advantages of the developed new AJR method have also been investigated. It has been found
475 that the J -R curves determined by the new AJR method are much closer to the accurate J -R
476 curve than those determined by UC and NM. As such the accuracy of the developed new AJR
477 method has been verified. It has also been found that the new AJR method should be the first
478 choice for materials with a small strain hardening ratio (or exponent) and low effective yield
479 strength, and thicker CT specimens with shallower initial crack length. This is because the
480 disagreement between UC and NM is unacceptably large. It can be concluded that the
481 developed new AJR method can determine the accurate J -R curve for steels with the required
482 accuracy.

483 **ACKNOWLEDGMENT**

484 Financial support from the Australian Research Council under DP140101547, LP150100413
485 and DP170102211, and the National Natural Science Foundation of China with Grant No.
486 51820105014 is gratefully acknowledged.

487 **AUTHOR CONTRIBUTIONS**

488 All authors contributed to the paper with the proportion in the order of the sequence of the
489 authorship. The work of the paper is supervised by the corresponding author.

490 **DATA AVAILABILITY STATEMENT**

491 Data that support the findings of this study are available from the corresponding author upon
492 reasonable request.

493 **REFERENCES**

- 494 1. ASTM E1820-18. *Standard test method for measurement of fracture toughness*. American
495 Society for Testing and Materials, 2018.
496
- 497 2. Anderson TL. *Fracture mechanics: fundamentals and applications*. CRC press; 2017.
498
- 499 3. Zhu X, Joyce J. Review of fracture toughness (G , K , J , CTOD, CTOA) testing and
500 standardization. *Eng Fract Mech*. 2012; 85: 1-46.
501
- 502 4. Clarke G, Andrews W, Paris P, Schmidt D. Single specimen tests for J_{Ic} determination. In:
503 *Mechanics of Crack Growth*, West Conshohocken, PA; ed. J. Rice and P. Paris, ASTM
504 STP 590; 1976, p.27-42.
505
- 506 5. B.S. 7448-4:1997. *Fracture mechanics toughness tests - part 4: method for determination*
507 *of fracture resistance curves and initiation values for stable crack extension in metallic*
508 *materials*. British Standards Institution, 1997.
509
- 510 6. Herrera R, Landes J. A direct J - R curve analysis of fracture toughness tests. *J Test Eval*.
511 1988; 16: 427-449.
512
- 513 7. Herrera R, Landes J. Direct J - R curve analysis: a guide to the methodology. In: *Fracture*
514 *mechanics: twenty-first symposium, West Conshohocken, PA*. ASTM STP 1074; 1990; 24-
515 43.
516
- 517
- 518
- 519 8. Orange T. Method and models for R-Curve instability calculations. In: *Fracture*
520 *mechanics: twenty-first symposium, West Conshohocken, PA*. ASTM STP 1074; 1990;
521 545-559.
522
- 523 9. Zhou Z, Lee K, Herrera R, Landes J. Normalization: an experimental method for
524 developing J - R curves, In: *Elastic-plastic fracture test methods: the user's experience*
525 *(second volume)*, West Conshohocken, PA. ASTM STP 1114; 1991; 42-56.
526
- 527 10. Landes J, Zhou Z, Lee K, Herrera R. Normalization method for developing J - R curves
528 with the LMN function, *J Test Eval*. 1991; 19: 305-311.
529
- 530 11. Scibetta M, Lucon E, Schuurmans J, Walle E. Numerical simulations to support the
531 normalization data reduction technique, *Eng Fract Mech*. 2006; 73: 524-534.
532

- 533 12. Joyce J. Analysis of a high rate round robin based on proposed annexes to ASTM E 1820.
534 *J Test Eval.* 2001; 29: 329-351.
535
- 536 13. Lee K, Landes J. Developing *J-R* Curves Without Displacement Measurement Using
537 Normalization. In: *Fracture mechanics: twenty-third symposium, West Conshohocken,*
538 *PA.* ASTM ATP1189; 1993; 133-167.
539
- 540 14. Bao C, Cai L, He G, Dan C. Normalization method for evaluating J-resistance curves of
541 small-sized CIET specimen and crack front constraints. *Int. J Solids Struct.* 2016; 94: 60-
542 75.
543
- 544 15. Cassanelli A, Ortiz H, Wainstein J. Separability property and load normalization in AA
545 6061-T6 aluminum alloy. In: *Fatigue and fracture mechanics: 32nd volume, West*
546 *Conshohocken, PA.* ASTM STP 1406; 2002; 49-72.
547
- 548 16. Landes J, Zhou Z. Application of load separation and normalization methods for
549 polycarbonate materials, *Int J Fract.* 1993; 63: 383-393.
550
- 551 17. Morhain C, Velasco J. Determination of *J-R* curve of polypropylene copolymers using the
552 normalization method. *J Mater Sci.* 2001; 36: 1487-1499.
553
- 554 18. Baldi F, Riccò T. High-rate J-testing of toughened polyamide 6/6: Applicability of the
555 load separation criterion and the normalization method. *Eng Fract Mech.* 2005; 72: 2218-
556 2231.
557
- 558 19. Varadarajan R, Dapp E, Rimnac C. Static fracture resistance of ultra high molecular
559 weight polyethylene using the single specimen normalization method. *Polym Test.* 2008;
560 27: 260-268.
561
- 562 20. Frontini P, Fasce L, Rueda F. Non linear fracture mechanics of polymers: Load
563 Separation and Normalization methods. *Eng Fract Mech.* 2012; 79: 389-414.
564
- 565 21. Dubey J, Wadekar S, Singh R, Sinha T, Chakravartty J. Assessment of hydrogen
566 embrittlement of Zircaloy-2 pressure tubes using unloading compliance and load
567 normalization techniques for determining J–R curves. *J Nucl Mater.* 1999; 264: 20-28.
568
- 569 22. Džugan J, Viehrig H. Application of the normalization method for the determination of *J–*
570 *R* curves. *Mater Sci Eng A.* 2004; 387: 307-311.
571
- 572 23. Zhu X, Joyce J. J–resistance curve testing of HY80 steel using SE (B) specimens and
573 normalization method. *Eng Fract Mech.* 2007; 74: 2263-2281.
574
- 575 24. Zhu X, Leis B. Fracture resistance curve testing of X80 pipeline steel using the SENB
576 specimen and normalization method. *J Pipeline Syst Eng.* 2008; 7.
577
- 578 25. Bao C, Cai L, Shi K, Dan C, Yao Y. Improved normalization method for ductile fracture
579 toughness determination based on dimensionless load separation principle. *Acta Mech*
580 *Solida Sin.* 2015; 28: 168-181.
581

- 582 26. He G, Bao C, Cai L, Wu Y, Zhao X. Estimation of J-resistance curves of SA-508 steel
583 from small sized specimens with the correction of crack tip constraint, *Eng Fract Mech.*
584 2018.
585
- 586 27. de Menezes J, Ipiña J. Castrodeza E. Normalization method for JR curve determination
587 using SENT specimens. *Eng Fract Mech.* 2018; 199: 658-671.
588
- 589 28. Gao H, Wu Y, Li C.-Q. Performance of normalization method for steel with different
590 strain hardening levels and effective yield strengths. *Eng Fract Mech.* 2019; 218.
591
- 592 29. Gao H, Wang W, Wang Y, Zhang B, Li C-Q. A modified normalization method for
593 determining fracture toughness of steel. *Fatigue Frac Eng Mat Struct.* 2020; 44: 568-583.
594
- 595 30. Gao H, Li C-Q, Wang W, Wang Y, Zhang B. Factors affecting the agreement between
596 unloading compliance method and normalization method. *Eng Fract Mech.* 2020; 235.
597
- 598 31. Wallin K, Laukkanen A. Improved crack growth corrections for J-R-curve testing. *Eng*
599 *Fract Mech.* 2004; 71: 1601-1614.
600
- 601 32. Fortes C, Bastian F. A modified normalization method for developing J-R and CTOD-R
602 curves with the LMN function. *J Test Eval.* 1997; 25: 302-307.
603
- 604 33. Landes J, McCabe D, Ernst H, Fracture testing of ductile steels. *NP-5014, Final report of*
605 *project 1238-2, Electric Power Research Institute, Palo Alto, CA, 1987.*
606
- 607 34. Landes J, McCabe D, Ernst H, Elastic-plastic methodology to establish R-curves and
608 instability criteria. *Final Report of Project EPRI RP1238-2, Electric Power Research*
609 *Institute, 1983.*
610
- 611 35. Zhu X, Lam P, Chao Y. Application of normalization method to fracture resistance
612 testing for storage tank A285 carbon steel. *Int J Pres Ves Pip.* 2009; 86: 669-676.
613
- 614 36. Joyce J, Gudas J, Computer Interactive J_{Ic} of Testing Navy Alloys. *Elastic-plastic*
615 *Fracture; 1979; ASTM STP 668: 451-468.*
616

617